# Electronic Supplementary Material

# Block copolymers as efficient cathode interlayer materials for organic solar cells

**Dingqin Hu[1], Jiehao Fu[1], Shanshan Chen[2], Jun Li[3], Qianguang Yang[1], Jie Gao[1], Hua Tang[1], Zhipeng Kan[1], Tainan Duan[1], Shirong Lu (✉)[1], Kuan Sun (✉)[2], Zeyun Xiao (✉)[1]**

1 Chongqing Institute of Green and Intelligent Technology, Chongqing School, University of Chinese Academy of Sciences (UCAS Chongqing), Chinese Academy of Sciences, Chongqing 400714, China

2 MOE Key Laboratory of Low-Grade Energy Utilization Technologies and Systems, School of Energy & Power Engineering, Chongqing University, Chongqing 400044, China

3 Library & Information Center, Anhui University of Finance and Economics, Bengbu 233030, China

E-mails: lushirong@cigit.ac.cn (Lu S); kuan.sun@cqu.edu.cn (Sun K); xiao.z@cigit.ac.cn (Xiao Z)

## Experimental Section

### 1. Materials

All reagents and solvents, unless otherwise specified, were purchased from Energy Chemical, Tansoole, Suna Tech, Aldrich and JiangSu GE-Chem Biotech. Ltd, and were used without further purification. PCE13 and IT-4Fwere purchased from Solarmer Energy Inc, P3HT and $PC_{61}BM$ were purchased from Luminescence Technology Corp，P1-P5 were purchased from Xi'an Ruixi Biological Technology Co. Ltd.

### 2. Thin film Characterizations

**i.** Ultraviolet−visible light (**UV-vis**) absorbance spectra were recorded on a Perkin Eimer Lambda 365 spectrophotometer. **Contact angle** was measured by DSA-100 (KRUSS Germany). **GPC** curves were obtained on OMNISEC.

**ii.** Thermogravimetric analysis (**TGA**) was carried out on a METTLER TOLEDO TGA/DSC 1 thermo gravimetric analyzer with thermal balance under protection of nitrogen at a heating rate of 10 °C $min^{-1}$, and differential scanning calorimetry (**DSC**) experiments

were performed on a METTLER TOLEDO DSC 1 differential scanning calorimeter with thermal balance under protection of nitrogen at a heating rate of 20 °C/$min^{-1}$. The work function of films were tested via ultraviolet photo emission spectroscopy (**UPS**) based on ESCAL ab 250Xi.

**iii.** Topographic images of the films were obtained from a Bruker atomic force microscopy (**AFM**) with the type of dimension edge with Scan AsystTM in the tapping mode using an etched silicon cantilever at a nominal load of ~2nN, and the scanning rate for a 2 μm×2 μm image size was 1.5 Hz. The thickness of P1-P5 films are also tested via AFM. C-AFM images were obtained with bias voltage from -10 V~10 V.

**iv.** Transmission electron microscope (**TEM**) studies were conducted with a Talos F200S electron microscopy to investigate the phase distribution of the active layer.

**v.** Grazing-Incidence wide-angle X-ray scattering (**GIWAXS**) measurements were carried out at 5A beamline of the Pohang Light Source II (PLS-II) in South Korea. The GIWAXS images were recorded at 0.13 incidence angle with X-rays of 11.57 keV (λ=1.0716Å) and MAR345 image plate detector.

## 3. ZnO preparation

The ZnO precursor was prepared by dissolving zinc acetate dihydrate ($Zn(CH_3COO)_2 \cdot 2H_2O$, Aldrich, 99.9%, 1 g) and ethanolamine ($NH_2CH_2CH_2OH$, Aldrich, 99.5%, 0.28 g) in 2-methoxyethanol ($CH_3OCH_2CH_2OH$, Aldrich, 99.8%, 10 mL) under vigorous stirring for 12 h for the hydrolysis reaction in air. The ZnO precursor solution was spin-cast on top of the ITO-glass substrate. The films were annealed at 200 ° C for 15 min in air.

## 4. The electron conductivity (EC) measurements

The longitudinal and horizontal EC was tested through sandwich structure, longitudinal EC based on structure of ITO/CIL/Ag, horizontal EC based on structure of Glass substrate/CIL/Ag, CIL including ZnO and five polymers (P1-P5), corresponding formula: GEC=L/RS, R is the resistance of P1-P5, S is the cross sectional area of electrodes measured, L is the length between electrodes measured.

**5. Current-density (*J*-*V*) and external quantum efficiency (*EQE*) measurements.**

The *J*-*V* of unencapsulated photovoltaic devices were measured under air using a Keithley 2400 source meter. A 300 W xenon arc solar simulator (Oriel) with an AM 1.5 global filter operated at 100 mW/cm$^2$ was used to simulate the AM 1.5G solar irradiation. The illumination intensity was corrected by using a silicon photodiode with a protective KG5 filter calibrated by the National Renewable Energy Laboratory (NREL). The EQE was performed using certified IPCE equipment (Zolix Instruments, Inc, Solar Cell Scan 100).

## Supporting Figures

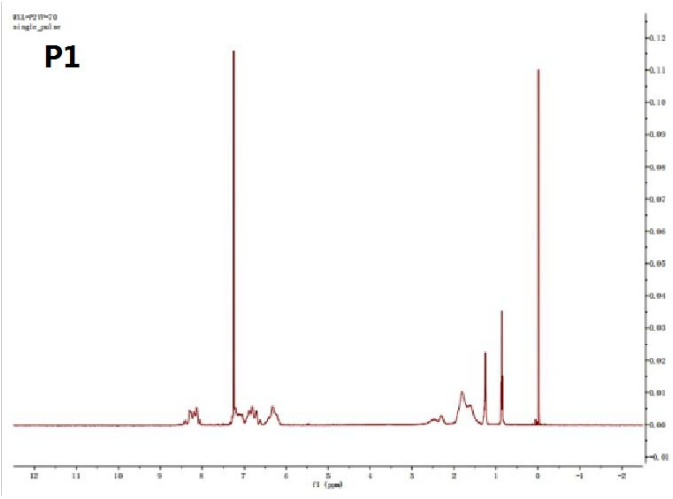

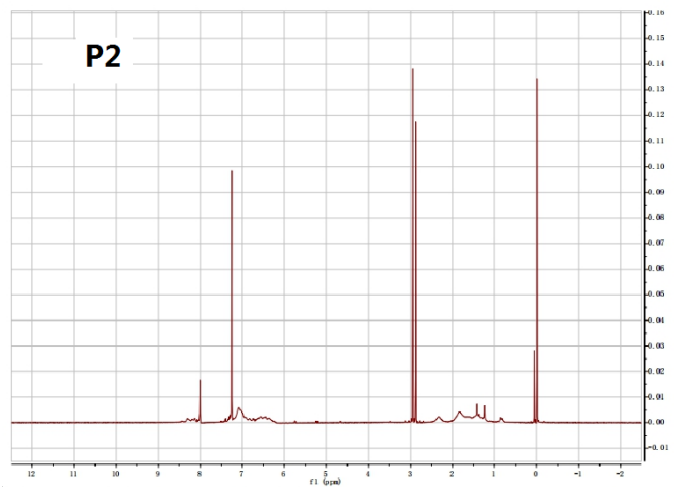
P2

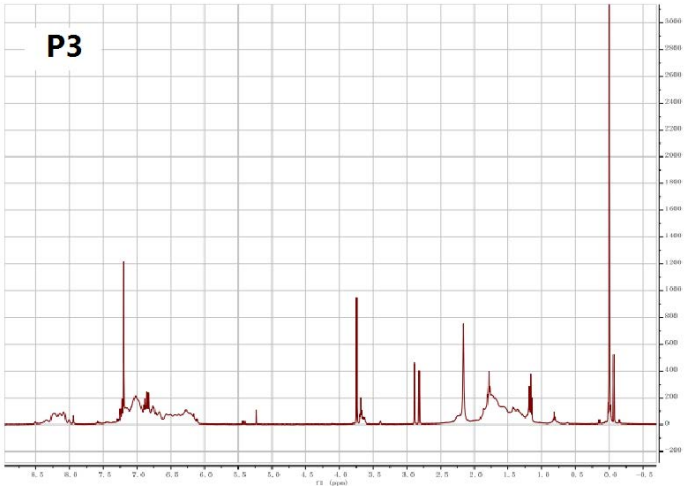
P3

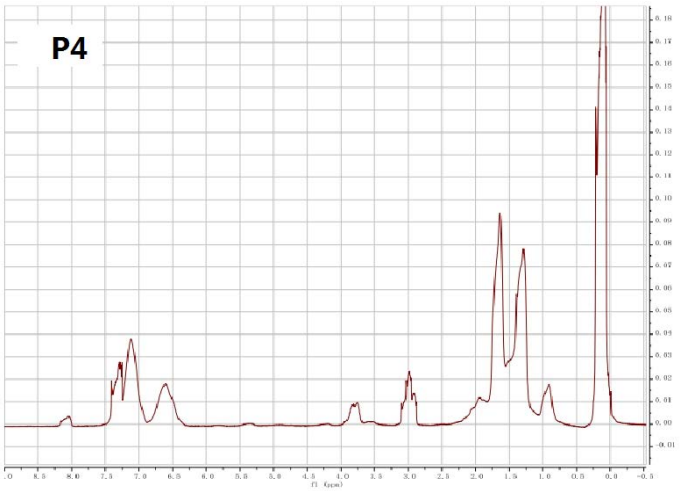
P4

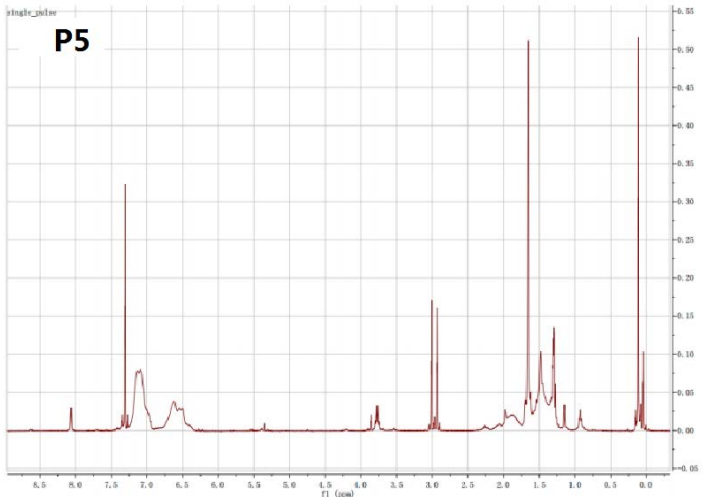


**Supplementary Figure S1** $^{1}$H NMR spectra of P1-P5.

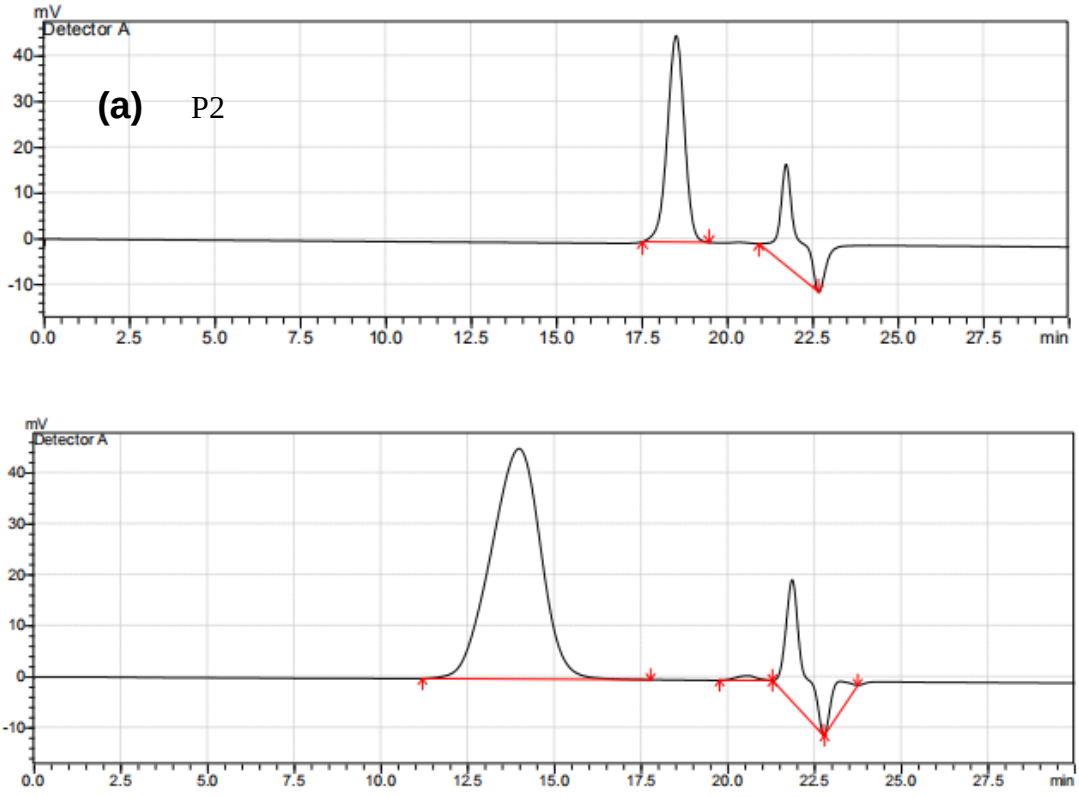

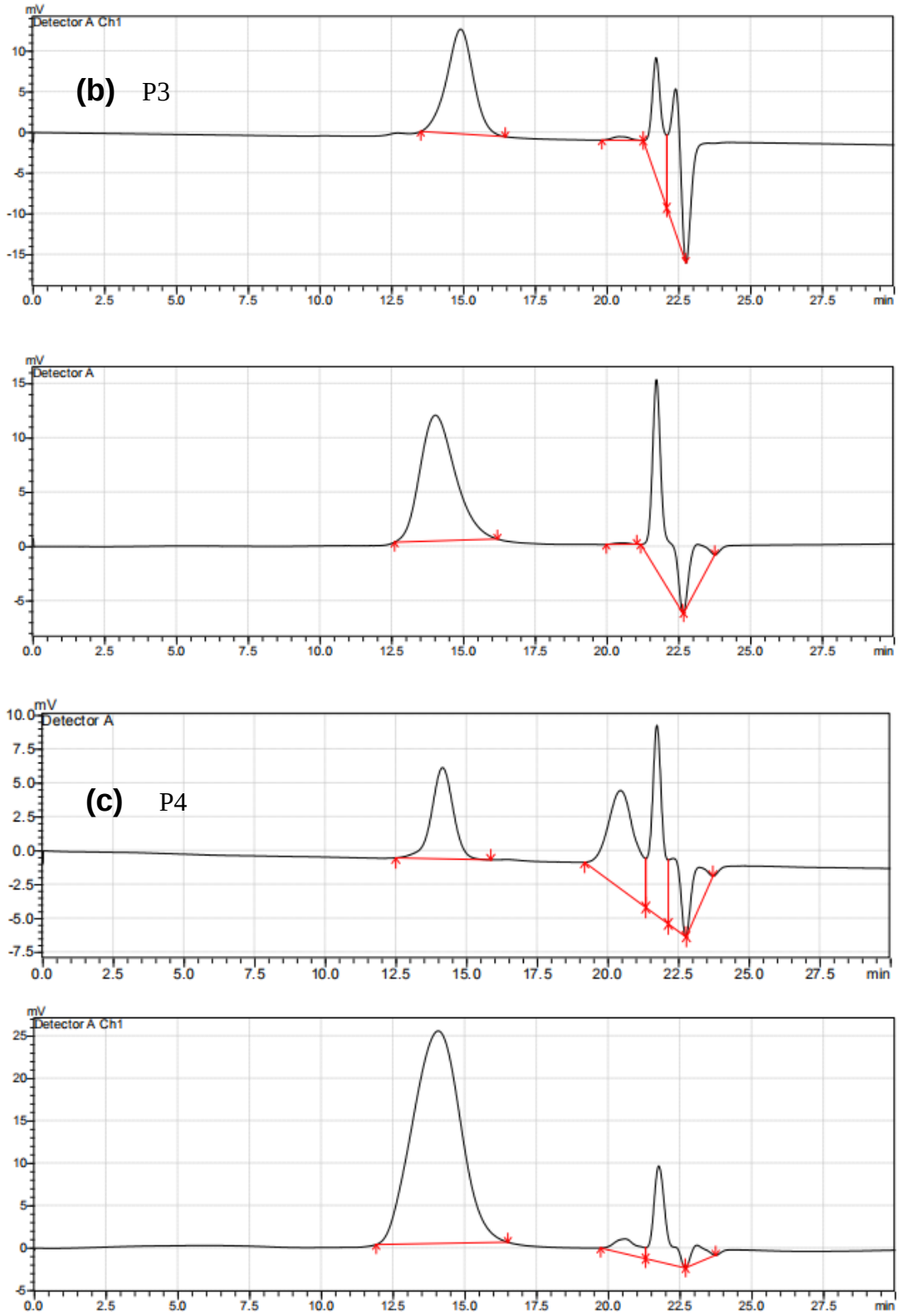


**Supplementary Figure S2 (a)~(c)** GPC diagrams of P2-P4, the upper diagrams in each of the figure are the GPC of PS block, the lower ones are the GPC of PS-*b*-P2VP.

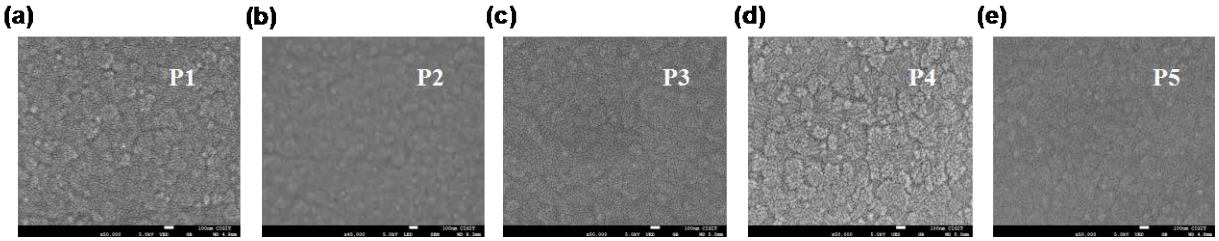


**Supplementary Figure S3 (a)~(e)** SEM images of the P1-P5 polymers.

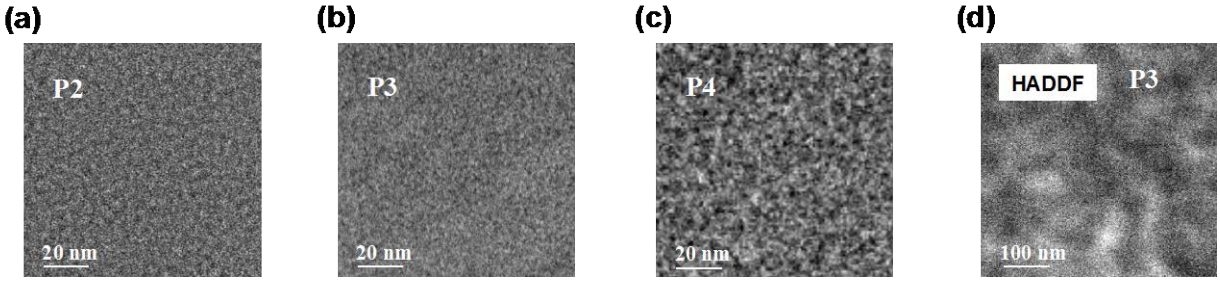


**Supplementary Figure S4 (a)~(c)** TEM images of the P2-P4 polymers.

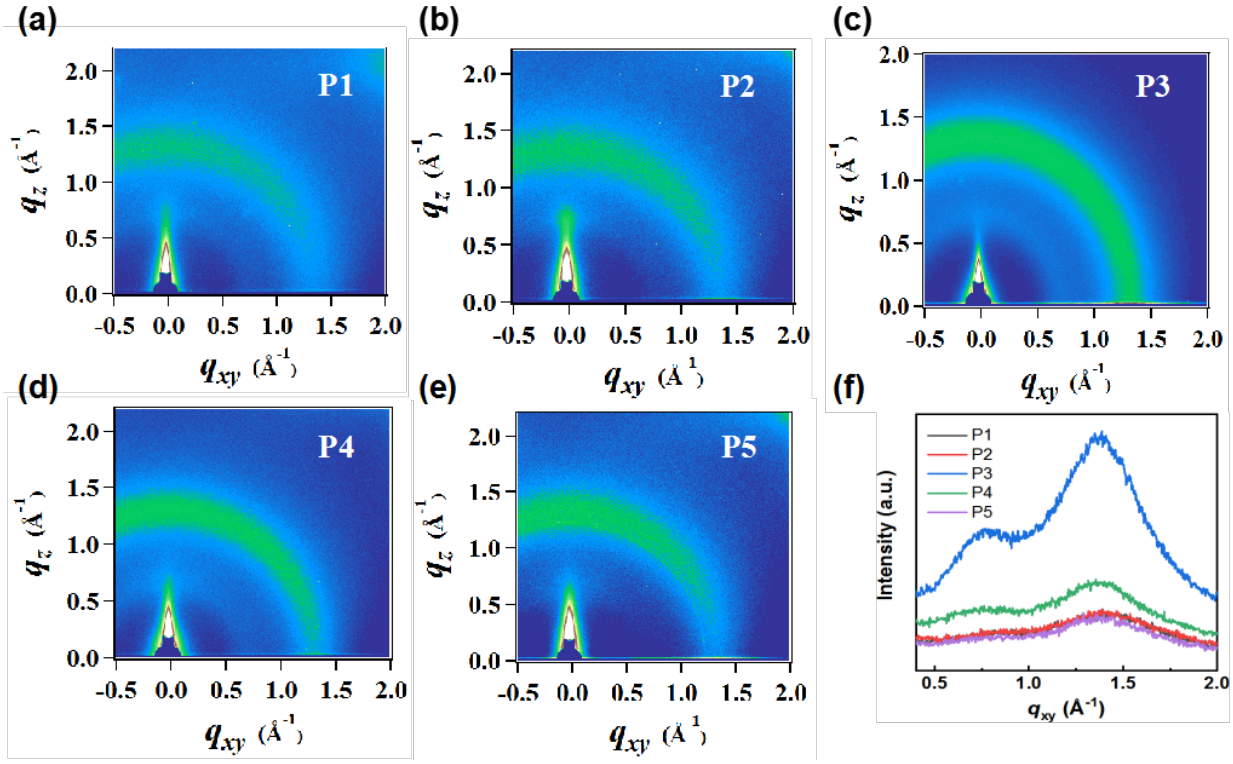


**Supplementary Figure S5 (a)~(e)** GIWAXS of the P1-P5 thin films on silicon wafer via spin-coating. **(f)** In-plane diffraction patterns of P1-P5 thin films .

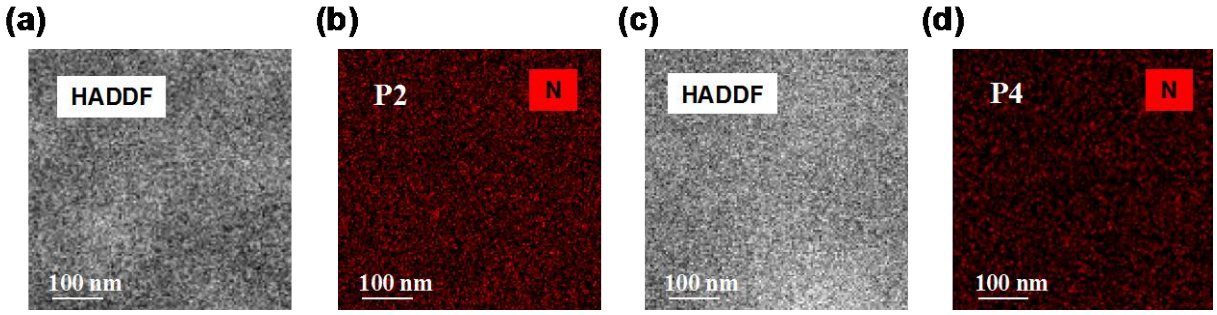


**Supplementary Figure S6 (a)** and **(c)** HADDF images of the P2 and P4 block copolymers. **(b)** and **(d)** EDS mapping (TEM mode) of the N components of the P2 and P4 block copolymers.

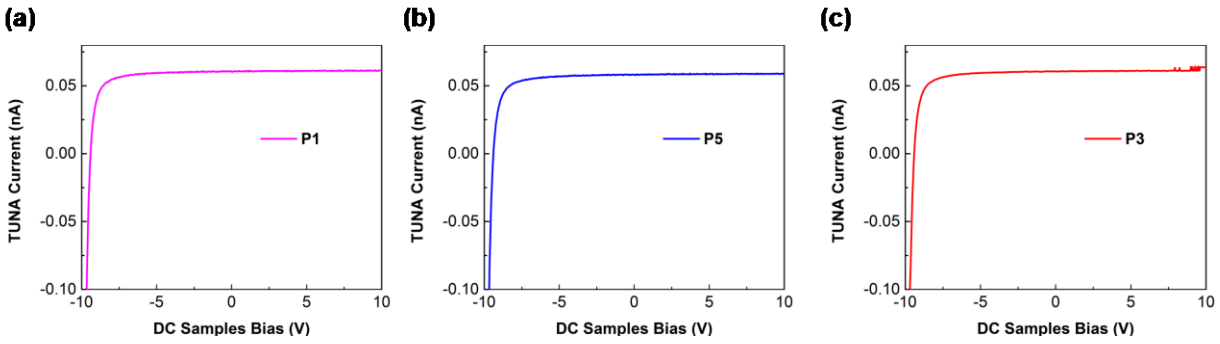


**Supplementary Figure S7 (a)~(c)** Bias-current curves of P1, P3 and P5 cathode interlayers via the measurement of C-AFM.

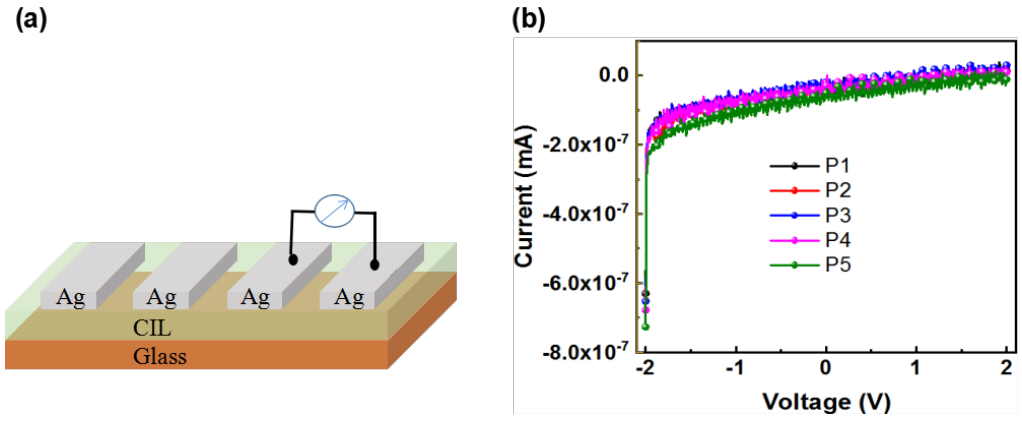


**Supplementary Figure S8 (a)** Sandwich structure to measure horizontal electron conductivity. **(b)** Current-voltage curves of the five polymer materials (P1-P5).

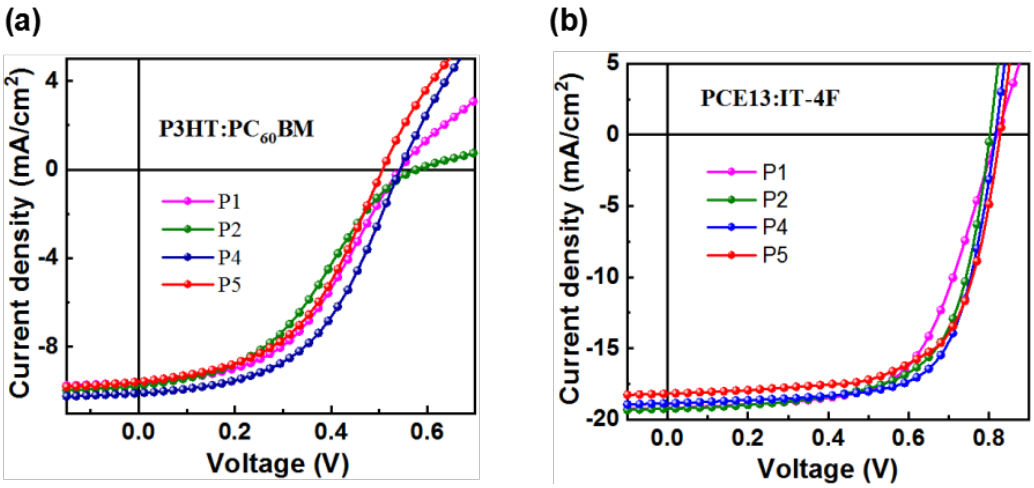


**Supplementary Figure S9** *J-V* curves of **(a)** P3HT:$PC_{61}BM$ and **(b)** PCE13:IT-4F based organic solar cells with P1, P2, P4, P5 cathode interlayers.

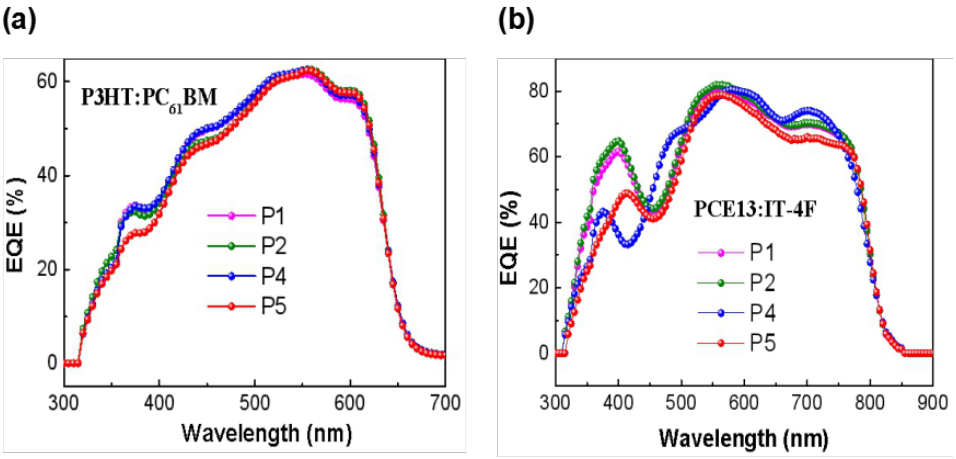


**Supplementary Figure S10** *EQE* curves of **(a)** P3HT:$PC_{61}BM$ and **(b)** PCE13:IT-4F based organic solar cells with P1, P2, P4, P5 cathode interlayers.

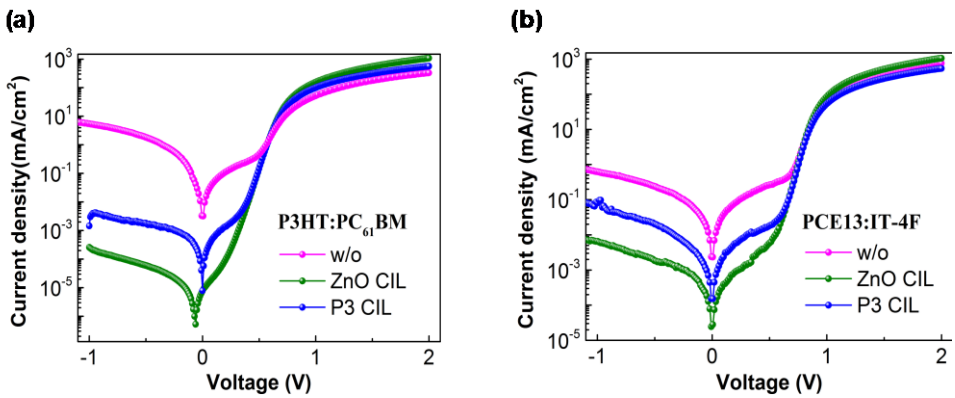

**Supplementary Figure S11** Dark current density (*J*-*V*) curves of **(a)** P3HT:$PC_{61}BM$ and **(b)** PCE13:IT-4F based organic solar cells w/o, with ZnO and P3 cathode interlayer.

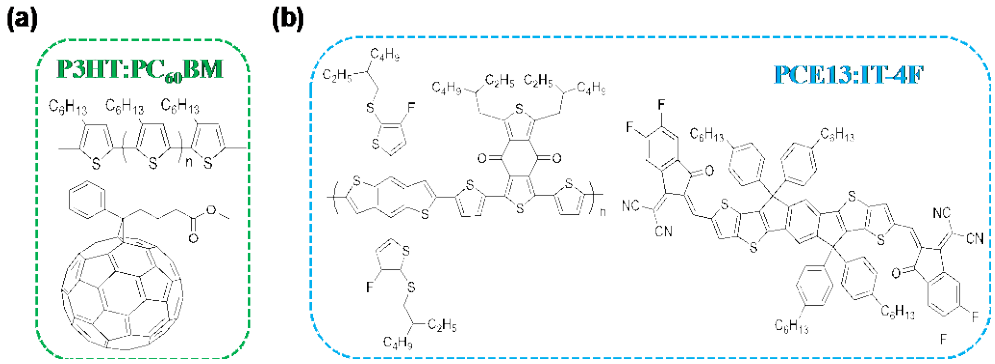


**Supplementary Figure S12 (a)** and **(b)** The chemical structure of P3HT, $PC_{61}BM$, PCE13 and IT-4F.

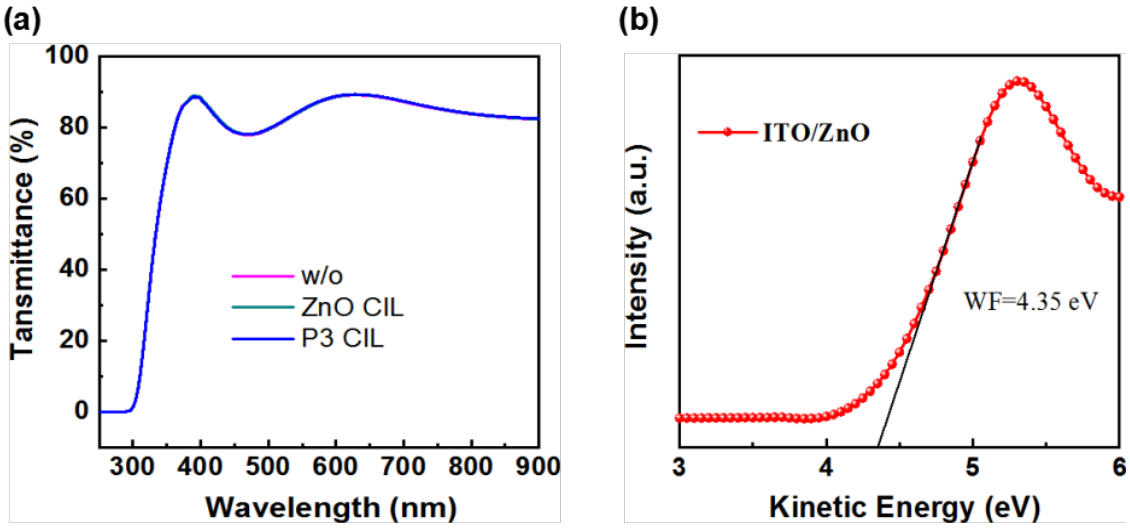


**Supplementary Figure S13 (a)** Transmittance curves of substrate, ZnO, P3 covered substrate. **(b)** UPS of ZnO cathode interlayer.

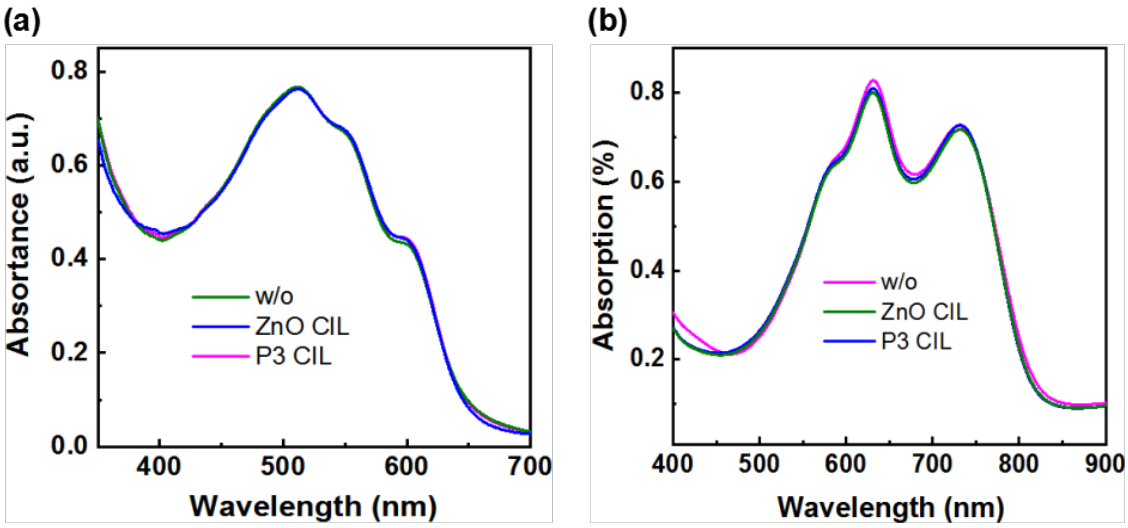


**Supplementary Figure S14** Absorption curves of **(a)** P3HT:$PC_{61}BM$ and **(b)** PCE13:IT-4F based organic solar cells w/o, with ZnO or P3 cathode interlayer.

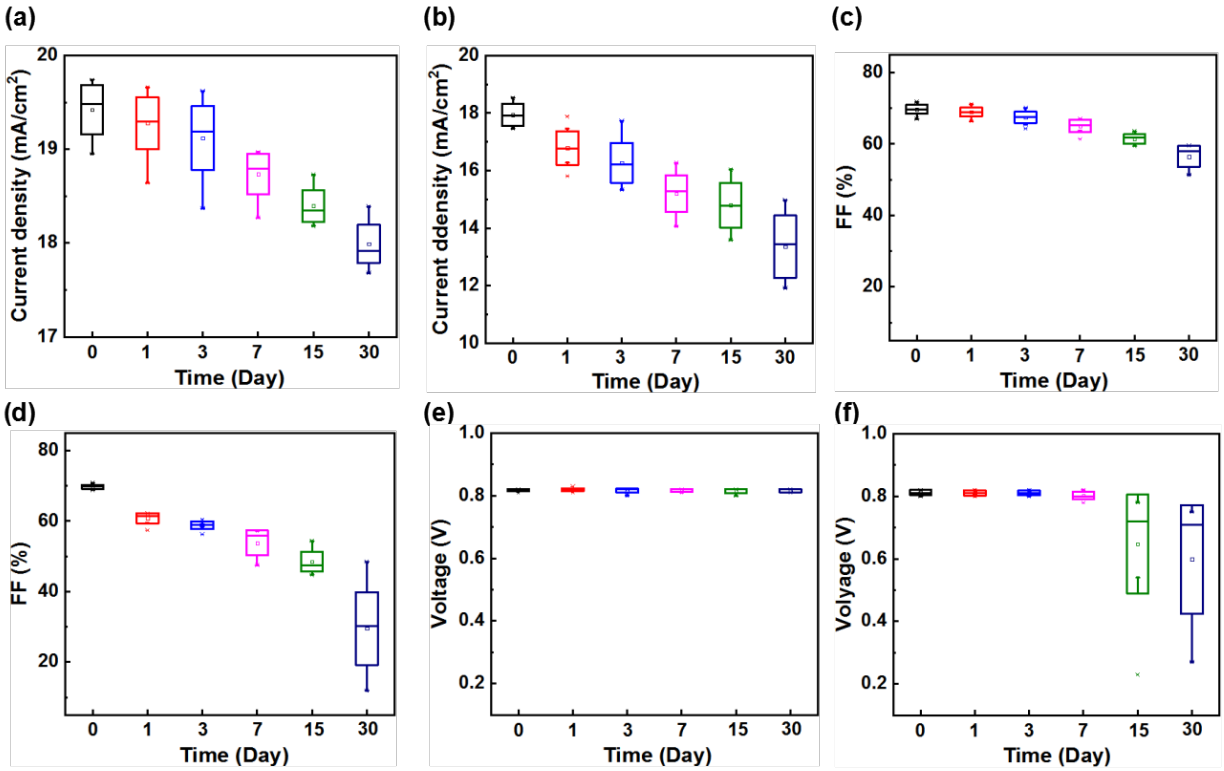


**Supplementary Figure S15** Voltage ($V_{oc}$) of PCE13:IT-4F-based OSCs in ambient atmosphere with humidity of 70% using with **(a)** P3 cathode interlayer and **(b)** ZnO cathode interlayer. Current density ($J_{sc}$) of PCE13:IT-4F-based OSCs in ambient atmosphere with humidity of

70% using with **(c)** P3 cathode interlayer and **(d)** ZnO cathode interlayer. Fill factor (*FF*) of PCE13:IT-4F-based OSCs in ambient atmosphere with humidity of 70% using with **(e)** P3 cathode interlayer and **(f)** ZnO cathode interlayer.

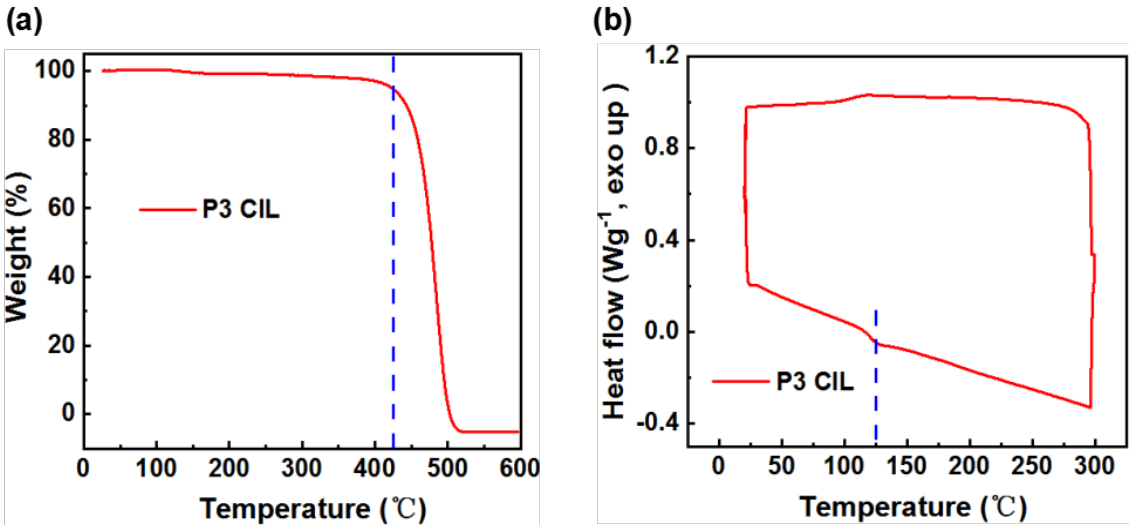


**Supplementary Figure S16 (a)** Thermo-gravimetric analysis and **(b)** Differential scanning calorimetry of P3 polymer.

## Supporting Tables

**Supplementary Table S1.** Analysis data of the two-dimensional GIWAXS results in out-of-plane direction (OOP).

| Film | Lattice plane | Peak location ($A^{-1}$) | | d-spacing (Å) | | FWHM ($A^{-1}$) | | Coherence length (Å) | |
|---|---|---|---|---|---|---|---|---|---|
| | | $q_{xy}$ | $q_z$ | $q_{xy}$ | $q_z$ | $q_{xy}$ | $q_z$ | $q_{xy}$ | $q_z$ |
| P1 | 010 | 1.382 | 1.368 | 4.548 | 4.593 | 0.557 | 0.486 | 10.221 | 11.722 |
| P2 | 010 | 1.404 | 1.363 | 4.477 | 4.611 | 0.609 | 0.578 | 9.360 | 9.852 |
| P3 | 010 | 1.374 | 1.373 | 4.571 | 4.577 | 0.499 | 0.389 | 11.409 | 14.646 |
| P4 | 010 | 1.366 | 1.345 | 4.601 | 4.672 | 0.507 | 0.511 | 11.230 | 11.152 |
| P5 | 010 | 1.434 | 1.360 | 4.383 | 4.619 | 0.540 | 0.588 | 10.556 | 10.204 |

**Supplementary Table S2.** Analysis data of the two-dimensional GIWAXS results in out-of-plane direction (IP).

| Film | Lattice plane | Peak location ($A^{-1}$) | d-spacing (Å) | FWHM ($A^{-1}$) | Coherence length (Å) |
|---|---|---|---|---|---|
| | | $q_{xy}$ | $q_{xy}$ | $q_{xy}$ | $q_{xy}$ |
| P1 | 100 | 0.684 | 9.189 | 0.384 | 14.747 |
| P2 | 100 | 0.801 | 7.840 | 0.375 | 15.133 |
| P3 | 100 | 0.750 | 8.377 | 0.309 | 18.325 |
| P4 | 100 | 0.707 | 8.887 | 0.450 | 12.601 |
| P5 | 100 | 0.827 | 7.593 | 0.536 | 10.575 |

**Supplementary Table S3.** Photovoltaic performance of P3HT:$PC_{61}BM$ and PCE13:IT-4F-based organic solar cells with P1, P2, P4, P5 cathode interlayer.

| Material | CIL | $V_{OC}$ [V] | $J_{SC}$ [mA/cm$^2$] | FF [%] | PCE Max [%] | [a)]Ave. PCE (%) | $J_{SC}$ [b)] [mA/cm$^2$] | *Rs* (Ω cm$^2$) | *Rsh* (Ω cm$^2$) |
|---|---|---|---|---|---|---|---|---|---|
| P3HT:$PC_{61}BM$ | P1 | 0.54(±0.01) | 9.61(±0.3) | 47.5(±0.4) | 2.44 | 2.27(±0.17) | 8.50 | 15.87 | $6.38\times10^4$ |
| | P2 | 0.58(±0.01) | 9.74(±0.4) | 39.0(±0.8) | 2.19 | 2.01(±0.18) | 8.49 | 18.59 | $1.26\times10^4$ |
| | P4 | 0.54(±0.01) | 10.09(±0.3) | 51.4(±0.7) | 2.77 | 2.59(±0.18) | 8.58 | 16.74 | $3.90\times10^5$ |
| | P5 | 0.51(±0.01) | 9.58(±0.3) | 48.5(±0.5) | 2.35 | 2.13(±0.23) | 8.37 | 16.82 | $5.91\times10^4$ |
| PCE13:IT-4F | P1 | 0.82(±0.01) | 19.19(±0.4) | 62.65(±0.7) | 9.83 | 9.68(±0.15) | 18.29 | 3.70 | $1.87\times10^4$ |
| | P2 | 0.82(±0.01) | 19.23(±0.4) | 65.09(±0.6) | 10.18 | 10.02(±0.16) | 18.48 | 2.84 | $2.53\times10^4$ |
| | P4 | 0.82(±0.01) | 18.87(±0.2) | 69.96(±1.0) | 10.79 | 10.33(±0.46) | 18.07 | 1.46 | $3.18\times10^4$ |
| | P5 | 0.83(±0.02) | 18.19(±0.2) | 67.04(±0.8) | 10.09 | 9.39(±0.70) | 17.23 | 2.05 | $2.86\times10^4$ |